THE JOURNAL OF BIOLOGICAL CHEMISTRY VOL. 288, NO. 31, pp. 22451–22459, August 2, 2013

Zebrafish Tyrosine Hydroxylase 2 Gene Encodes Tryptophan Hydroxylase*

Received for publication, May 16, 2013, and in revised form, June 5, 2013 Published, JBC Papers in Press, June 10, 2013, DOI 10.1074/jbc.M113.485227

Guiqi Ren[‡], Song Li[‡], Hanbing Zhong[‡], and Shuo Lin[‡§1]

From the [‡]Laboratory of Chemical Genomics, School of Chemical Biology and Biotechnology, Peking University Shenzhen Graduate School, Shenzhen 518055, China and the [§]Department of Molecular, Cell and Developmental Biology, UCLA, Los Angeles, California 90095

Background: Zebrafish tyrosine hydroxylase 2 (*th2*) has been considered as a marker of dopaminergic (DA) neurons in the investigation of DA neuron development and the pathological mechanism of Parkinson disease.
Results: *th2* is required for the synthesis of serotonin *in vivo* and has tryptophan hydroxylase activity *in vitro*.
Conclusion: *th2* should be considered as a marker gene of serotonergic neurons.
Significance: This result facilitates the elucidation of zebrafish neural circuitry.

The primary pathological hallmark of Parkinson disease (PD) is the profound loss of dopaminergic neurons in the substantia nigra pars compacta. To facilitate the understanding of the underling mechanism of PD, several zebrafish PD models have been generated to recapitulate the characteristics of dopaminergic (DA) neuron loss. In zebrafish studies, tyrosine hydroxylase 1 (*th1*) has been frequently used as a molecular marker of DA neurons. However, *th1* also labels norepinephrine and epinephrine neurons. Recently, a homologue of *th1*, named tyrosine hydroxylase 2 (*th2*), was identified based on the sequence homology and subsequently used as a novel marker of DA neurons. In this study, we present evidence that *th2* co-localizes with serotonin in the ventral diencephalon and caudal hypothalamus in zebrafish embryos. In addition, knockdown of *th2* reduces the level of serotonin in the corresponding *th2*-positive neurons. This phenotype can be rescued by both zebrafish *th2* and mouse tryptophan hydroxylase 1 (*Tph1*) mRNA as well as by 5-hydroxytryptophan, the product of tryptophan hydroxylase. Moreover, the purified Th2 protein has tryptophan hydroxylase activity comparable with that of the mouse TPH1 protein *in vitro*. Based on these *in vivo* and *in vitro* results, we conclude that *th2* is a gene encoding for tryptophan hydroxylase and should be used as a marker gene of serotonergic neurons.

Parkinson disease (PD)[2] is a common neurodegenerative disorder caused by progressive neuronal loss, primarily the degeneration of dopaminergic neurons in the substantia nigra pars compacta (1–3). The functions of dopaminergic neurons and the neural transmitter dopamine have been extensively studied (4). Tyrosine hydroxylase (TH) has been considered and widely used as a molecular marker of dopaminergic neurons because it is the entry and rate-limiting enzyme of dopamine synthesis. Several mammalian TH antibodies have been raised.

Zebrafish, an established vertebrate model for investigating human diseases, has been increasingly used to study PD (5–20). Although the evolutionary distance between humans and zebrafish is about 350 million years, the TH antibodies have cross-species immunoreactivity in zebrafish and can label the ascending dopaminergic system, which is considered as the counterpart of the human nigro-striatal dopamine system (21, 22). Although most of the diencephalic neurons project to the spinal cord (23), the alteration of DA neurons located in the posterior tuberculum of diencephalon has been used as an index marker to study zebrafish PD models (11, 13–15, 17–20, 24).

Two tyrosine hydroxylase genes have been reported in zebrafish. Both genes were cloned based on sequence homology, so they were named tyrosine hydroxylase 1 (*th1*; Gene ID 30384) and *tyrosine hydroxylase 2* (*th2*; Gene ID 414844), respectively (25). Zebrafish *th1* is more similar to mammalian *th* than *th2*. The pattern of immunostaining of TH antibody largely overlaps with that of whole mount RNA *in situ* hybridization using the zebrafish *th1* antisense RNA probe but not *th2*, indicating that the TH antibody preferentially reacts with zebrafish Th1 and not (or only little) with Th2 in the embryo (26). Similar results were obtained for three other tyrosine hydroxylase antibodies against mammalian TH protein (27–29). In addition, in the adult zebrafish, other DA neuron markers (L-3,4-dihydroxyphenylalanine (L-DOPA) decarboxylase (*ddc*; Gene ID 406651), vesicle monoamine transporter 2 (*vmat2*; Gene ID 553304), dopamine transporter (*dat*; Gene ID 80787), and dopamine) can only be detected in some but not all *th2*-positive neurons (28, 29). Based on these results, we reasoned that *th2* should not be considered as a tyrosine hydroxylase gene merely based on sequence homology. When surveying literature, we noticed that the expression patterns of *th2* and

* This work was supported by Ministry of Science and Technology of China Grants 2009CB941200 and 2009CB941300; Shenzhen Science and Technology Program Grants JC201104220257A, JC201005270280A, ZYC201006170364A, and GJHS20120628101219328; and Guangdong Natural Science Foundation Grant S2012010009028.
[1] To whom correspondence should be addressed: Life Sciences Bldg., 621 Charles E. Young Dr. S., Los Angeles, CA 90095. Tel.: 310-267-4970; Fax: 310-267-4971; E-mail: shuolin@ucla.edu.
[2] The abbreviations used are: PD, Parkinson disease; hpf, hours postfertilization; dpf, days postfertilization; 5-HT, 5-hydroxytryptamine, serotonin; 5-HTP, 5-hydroxytryptophan; DA, dopaminergic; DOPA, L-3,4-dihydroxyphenylalanine; MO, mopholino-oligonucleotide; EGFP, enhanced green fluorescent protein; L-DOPA, L-3,4-dihydroxyphenylalanine.

TABLE 1
Injection doses

MOs	MO dose/embryo	mRNA	mRNA dose/embryo	MO + mRNA	Dose/embryo
	ng		*pg*		*ng + pg*
ATG MO	1, 2, 4	*th1*	100, 200	ATG MO + *p53* MO + *th1* mRNA	4 + 4 + 200
p53 MO	2, 4, 8	NA[a]	NA	NA	NA
ATG MO + *p53* MO	2 + 4, 4 + 4, 8 + 4	*th2*	100, 200	ATG MO + *p53* MO + *th2* mRNA	4 + 4 + 100
Splicing MO	4, 8, 12, 16	Mouse *Tph1*	100, 200	ATG MO + *p53* MO + mouse *Tph1* mRNA	4 + 4 + 100
				Splicing MO + *th1* mRNA	12 + 200
				Splicing MO + *th2* mRNA	12 + 100
				Splicing MO + mouse *Tph1* mRNA	12 + 100

[a] NA, not applicable.

the neural transmitter serotonin share striking similarity in diencephalon (30). We therefore initiated experiments to investigate if *th2* is involved in 5-HT synthesis.

Here we show that *th2* co-localizes with 5-HT in ventral diencephalon and caudal hypothalamus. Knockdown of *th2* by mopholino-oligonucleotides (MOs) causes significant reduction of 5-HT in the corresponding *th2*-positive neurons, which can be rescued by both the mouse tryptophan hydroxylase 1 (*Tph1*; Gene ID 21990) and the product of tryptophan hydroxylase, 5-hydroxytryptophan (5-HTP). Moreover, the purified zebrafish Th2 protein has tryptophan hydroxylase activity comparable with that of the mouse TPH1 protein *in vitro*. Based on these findings, we suggest that *th2* should be considered as a gene encoding tryptophan hydroxylase and used as a marker for serotonergic neurons.

EXPERIMENTAL PROCEDURES

Zebrafish Husbandry—Wild type *Tuebingen* and the transgenic line *ETvmat2:GFP* (31) were raised in a recirculating aquaculture system according to *The Zebrafish Book* (32). Embryos were incubated at 28.5 °C and staged following Kimmel *et al.* (33). At 22–24 h postfertilization (hpf), embryos were treated with 1-phenyl-2-thiourea (Sigma-Aldrich) at a final concentration of 0.003% to prevent the pigmentation. The usage of zebrafish in this study was approved by Peking University Shenzhen Graduate School.

Design and Validation of MOs—Two MOs (ATG MO and splicing MO) of *th2* were purchased from Gene Tools Inc. (Philomath, OR). The sequence of the ATG MO was 5′-TCTGCGCTATACTGTCCGACTTCAT-3′. The sequence of the splicing MO was 5′-GCAGTCACAAAATCACCTACTCTTT-3′, which targeted the boundary of exon 2 and intron 2-3. The sequence of *p53* MO was described by Langheinrich *et al.* (34). The MOs were injected at the one-cell stage, as described by Ren *et al.* (20), with corresponding doses indicated in the figure legends and Table 1.

For validation of the ATG MO, an EGFP fused with ATG MO target site was generated. The primers used were 5′-GGATCCATGAAGTCGGACAGTATAGCGCAGAATGTGAGCAAGGGCGAGGA-3′ and 5′-CTCGAGTTACTTGTACAGCTCGTCCA-3′. This PCR product was cloned into a pCS2+ plasmid. 200 pg of this EGFP fusion construct and/or 1 ng of the ATG MO were injected at one-cell stage. At 6–8 hpf, the expression of GFP was observed under a fluorescent microscope (Zeiss).

For validation of the splicing MO, at 3 and 4 dpf, total RNA was extracted with the RNAqueous®-4PCR kit (Ambion, Austin, TX), and cDNAs were generated with the PrimeScript™ RT reagent kit (Takara, Dalian, China). Primers flanking target site were 5′-CGGAGACAGCTTCGTGTT-3′ and 5′-GCTCATTAGAAAGGGCATA-3′. The PCR products were cloned into a pGEM-T easy vector (Promega, Madison, WI) for sequencing.

TABLE 2
Doses of chemicals

Chemicals	Dose	Phenotype at 3 dpf
	μM	
5-HTP	22.7, 45.4, 90.8	30 embryos alive and morphologically normal in each group
L-DOPA	25.35, 50.7, 101.4	30 embryos alive and morphologically normal in each group

mRNA Synthesis and Injection—The cDNAs of *th1* and *th2* were cloned from total RNA of 3 dpf embryos. For the *th2* mRNA, a 6-base pair mismatch (underlined) in the ATG MO target site was introduced by the primers 5′-ATTTTCGATGAAGTC*CG*A*TTCG*AT*C*GCGCAGAATGTTCCG-3′ and 5′-CGGAACATTCTGCGCGATCGAATCGGACTTCATCGAAAAT-3′ using the template of the pCS2+ vector containing the original *th2* cDNA. Mouse *Tph1* was cloned from a nude BALB/c strain. All of the *th1*, *th2*, and mouse *Tph1* cDNAs were cloned into pCS2+ vector, and mRNAs were produced by the mMESSAGE mMACHINE® kit (Ambion, Austin, TX) and purified by the RNeasy® minikit (Qiagen, Hilden, Germany). The mRNA was injected alone or after the injection of the MO at corresponding doses, as indicated in the figure legends and Table 1.

Chemical Treatment—The embryos were dechorionated manually at 24 hpf and arrayed into a 6-well plate, 10 embryos/well in Holtfreter's buffer with 0.003% 1-phenyl-2-thiourea. L-DOPA and 5-HTP (Sigma-Aldrich) were added at 24 hpf with the concentrations shown in the legend of Fig. 4 and Table 2. The solution was replaced at 2 dpf.

Tryptophan Hydroxylase Activity and Tyrosine Hydroxylase Activity—The coding sequences of *th1*, *th2*, and mouse *Tph1* and *Th* were cloned into pGEX-6p-1 vector. The protein expression and purification procedure essentially followed Yohrling *et al.* (35). The expressed proteins in *Escherichia coli* were purified by glutathione-Sepharose beads (GE Healthcare). SDS-PAGE followed by Coomassie Brilliant Blue staining was used to confirm the expression of each protein. After protein quantification by Bradford method, the activity of each protein was measured by a tryptophan hydroxylase activity detection kit and a tyrosine hydroxylase activity detection kit (Genmed,

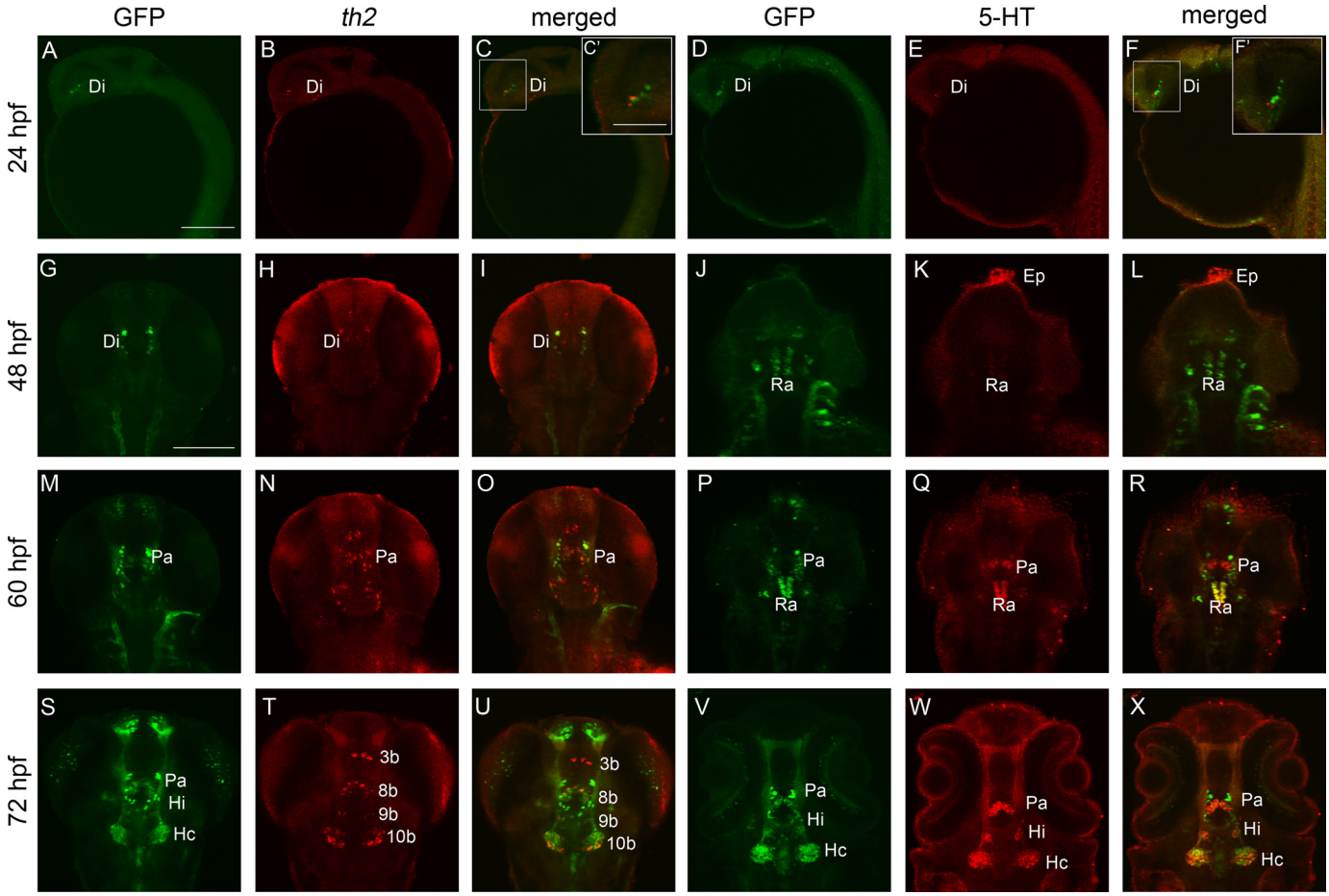

FIGURE 1. **Temporal and spatial localization analysis of *th2* and 5-HT shows that they co-localize in the ventral diencephalon and caudal hypothalamus at 72 hpf.** *A–F*, 24-hpf embryo, *lateral view*, anterior to the *left*. *A–C* show that *th2* expresses at close proximity with GFP of *ETvmat2:GFP* in the diencephalon. *C′* shows a *magnification* of the *white box* in *C*; *D–F* indicate that 5-HT also localizes at close proximity with the GFP in the diencephalon. *F′* shows a *magnification* of *white box* in *F*. *G–L*, 48-hpf embryo, *dorsal view*, anterior to the *top*. *G–I* show that *th2* expresses in three clusters of neurons but not with the GFP in the diencephalon; *J–L* show that 5-HT localizes in the epiphysis, and a weak level of 5-HT can be detected in the raphe nucleus. *M–R*, 60-hpf embryo, dorsal view, anterior to the top. *M–N* show that *th2* co-expresses with the GFP in the neural cluster of paraventricular organ (*Pa* in *M–O*). *P–R* show that 5-HT also co-localizes with the GFP in the neural cluster of the paraventricular organ (*Pa* in *P–R*). *S–X*, 72-hpf embryo, *dorsal view*, anterior to the *top*. *S–U*, GFP immunochemistry and *th2* fluorescent *in situ* hybridization show that there are four clusters of *th2*-positive neurons, 3b, 8b, 9b, and 10b in *T*; three of them co-localize with GFP in neural cluster of paraventricular organ, intermediate hypothalamus neural cluster (*Hi*), and caudal hypothalamus neural cluster (*Hc*) (*S* and *X*); *V–X*, GFP and 5-HT immunochemistry shows that 5-HT co-localizes with the same GFP-immunoreactive neurons of paraventricular organ, intermediate hypothalamus, and caudal hypothalamus. *Di*, neural cluster of diencephalon; *Ep*, neural cluster of epiphysis; *Ra*, neural cluster of raphe nucleus. *Scale bar*, 200 μm (*A–F*), 100 μm (*C′* and *F′*), and 100 μm (*G–X*).

Shanghai, China), respectively, following the instructions of the manufacturer.

Whole Mount Fluorescent in Situ Hybridization and Immunohistochemistry—Primers for *th2* probe synthesis were 5′-CGGAGACAGCTTCGTGTT-3′ and 5′-GCTCATTAGAAAGGGCATA-3′. PCR product was cloned into a pGEM-T easy vector (Promega). After linearization by SpeI, probe is produced by T7 RNA polymerase (Promega). The whole mount fluorescent *in situ* hybridization was performed essentially as described by Brend and Holley (36) and Flinn *et al.* (14). In the combination with GFP antibody staining, a rabbit anti-GFP antibody (1:500; Proteintech, Chicago, IL) was co-incubated with an anti-digoxigenin-peroxidase antibody (1:1000; Roche Applied Science) at 4 °C overnight. After detection of *th2* by the Cy3 TSA Plus system kit (PerkinElmer Life Sciences), an Alexa Fluor® 488-conjugated goat anti-rabbit second antibody (1:200; Invitrogen) was added at 4 °C overnight.

For 5-HT and GFP co-staining, a rabbit anti-5-HT (1:500; Sigma-Aldrich) and a mouse anti-GFP antibody (1:1000; Invitrogen) co-incubated at 4 °C overnight. After washing with blocking solution (1% blocking reagent (Roche Applied Science) plus 5% goat serum in PBST), a Cy3-labeled goat anti-rabbit second antibody (1:200; Proteintech) and an Alexa Fluor® 488-conjugated goat anti-mouse second antibody (1:200; Invitrogen) were added.

Imaging—Pictures of zebrafish embryos were taken with a Zeiss LSM 510 meta confocal microscope. The microscopist was single-blinded. The signals of raphe nucleus were intentionally overexposed to allow detection of all signals in 8b, 9b, and 10b regions in a linear range. The 5-HT level was semi-quantified by the gray level of the signal (regions of interest indicated in Fig. 4*A*), and signals in 8b, 9b, and 10b neurons were normalized to the hypothalamic region immediately anterior to the raphe nucleus as an internal reference for each

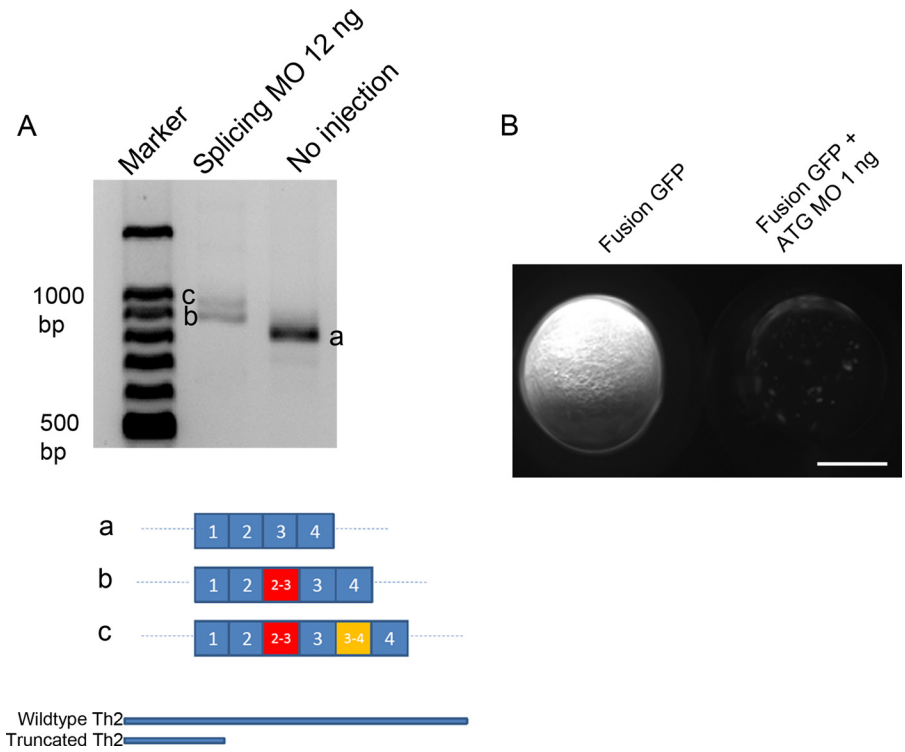

FIGURE 2. **Verification of splicing MO and ATG MO.** *A*, RT-PCR shows altered mRNA product (*b* and *c*) in the 12-ng splicing MO group. *Bottom*, schematic representation of the sequencing result shows that there is intron 2-3 insertion in *b*; there is intron 2-3 and intron 3-4 insertion in *c*. *Bottom*, schematic representation shows that both of the altered mRNA products will generate the same very short truncated protein product. *B*, strong GFP appeared in embryos injected with ATG MO target site fusion EGFP but not in embryos co-injected with ATG MO target site fusion EGFP and 1 ng of ATG MO. A *lateral view* is shown, anterior to the *top*. *Scale bar*, 250 μm.

image, as shown by a fixed size oval circle (Fig. 4*A*, *arrow*). Pictures were edited with Photoshop CS5 (Adobe Systems, San Jose, CA).

Statistical Analysis—All data had a normal distribution as validated by D'Agostino's test using StatPlus software (AnalystSoft Inc., Vancouver, Canada). All statistical analysis was performed with SPSS (IBM, Armonk, NY). All of the comparisons were performed by one-way analysis of variance, followed by a Tukey honestly significant difference pairwise comparison post hoc test. *Error bars* represent S.E. The numbers of embryos used are shown in the corresponding figure legends. *p* value less than 0.05 was considered as significant. All of the experiments were independently replicated at least three times.

RESULTS

5-HT and th2 Are Co-localized in the Ventral Diencephalon and Caudal Hypothalamus—As reported, 5-HT distributes in almost all brain regions, whereas in embryos, there are three major clusters of 5-HT-positive neurons in the diencephalon, which are the ventral part of the posterior tuberculum, the intermediate hypothalamus, and the caudal most aspect of the hypothalamus (30). *th2* is expressed in the preoptic region (3b), the anterior part of the paraventricular organ (8b), the intermediate part of the paraventricular organ (9b), and the posterior part of the paraventricular organ (10b) during embryogenesis (17, 26). Despite different nomenclature of the neuron clusters, there is striking similarity between the patterns of 5-HT and *th2*.

Direct co-staining of *th2* RNA *in situ* hybridization and 5-HT immunohistochemistry failed, probably because 5-HT is a small molecule, and the high temperature hybridization step of *in situ* hybridization destroyed its endogenous distribution. Therefore, we needed an "intermediate" reference marker to compare the expression patterns of *th2* and 5-HT. The candidate marker genes include *ddc*, *vmat2*, *dat*, and serotonin transporter. In embryos, *dat* and serotonin transporter have not been found to express in these regions, although *dat* is expressed at the hypothalamus in adult (28). *ddc* is expressed in the *th2*-positive areas in adult (27–29, 37), but its expression in embryos is restricted to the caudal tuberculum dopaminergic neuron and hindbrain raphe nucleus (14), where *th2* is not expressed. In contrast, *vmat2* is expressed in the diencephalon with a similar pattern of both *th2* and 5-HT (17, 26, 30, 31). We therefore selected *vmat2* as the marker gene to determine co-localization of *th2* and 5-HT. To circumvent the difficulty of direct co-staining of *in situ* hybridization and 5-HT immunohistochemistry, we used an *ETvmat2*:*GFP* transgenic line in which *vmat2*-positive neurons are labeled with GFP (31). We performed immunohistochemistry detection of GFP, avoiding the loss of 5-HT caused by high temperature, so the expression of GFP could serve as an intermediate reference marker to examine whether *th2* and 5-HT co-localize.

We found that *th2* was expressed in diencephalon from 24 hpf onward (Fig. 1, *B* and *C*), preceding the expression of GFP and the appearance of 5-HT before 60 hpf (Fig. 1, *Q* and *R*). At 72 hpf, three pairs of GFP-immunoreactive neurons appeared in neural clusters of paraventricular organ (*Pa*), intermediate hypothalamus neural cluster (*Hi*), and caudal hypothalamus neural cluster (*Hc*), as

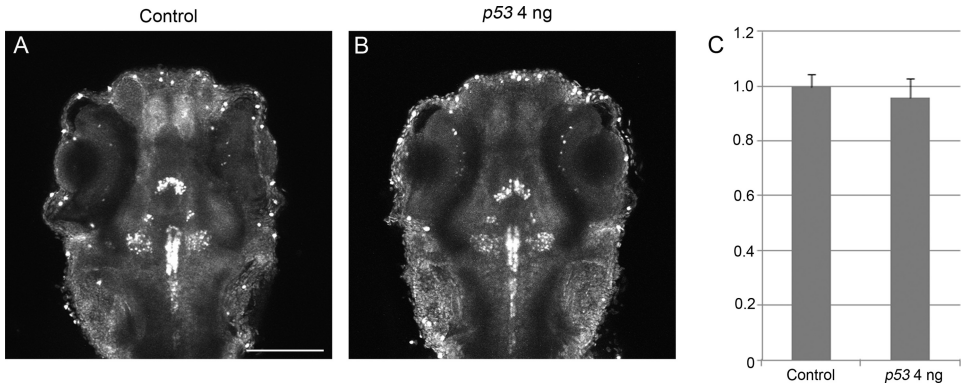

FIGURE 3. **Knockdown of *p53* does not cause decrease of 5-HT in 8b, 9b, and 10b neurons.** A *dorsal view* is shown, anterior to the *top*. *A* and *B*, *Z*-stack (70-μm) images of 5-HT immunoreactivity of 72-hpf embryos. *A*, control; *B*, *p53* MO 4 ng. *C*, statistical result shows that the 5-HT level is not significantly different between control and the *p53* morphant group ($p = 0.85$). The *y* axis shows relative 5-HT level. $n = 20$ in each group; *error bars*, S.E. *Scale bar*, 100 μm.

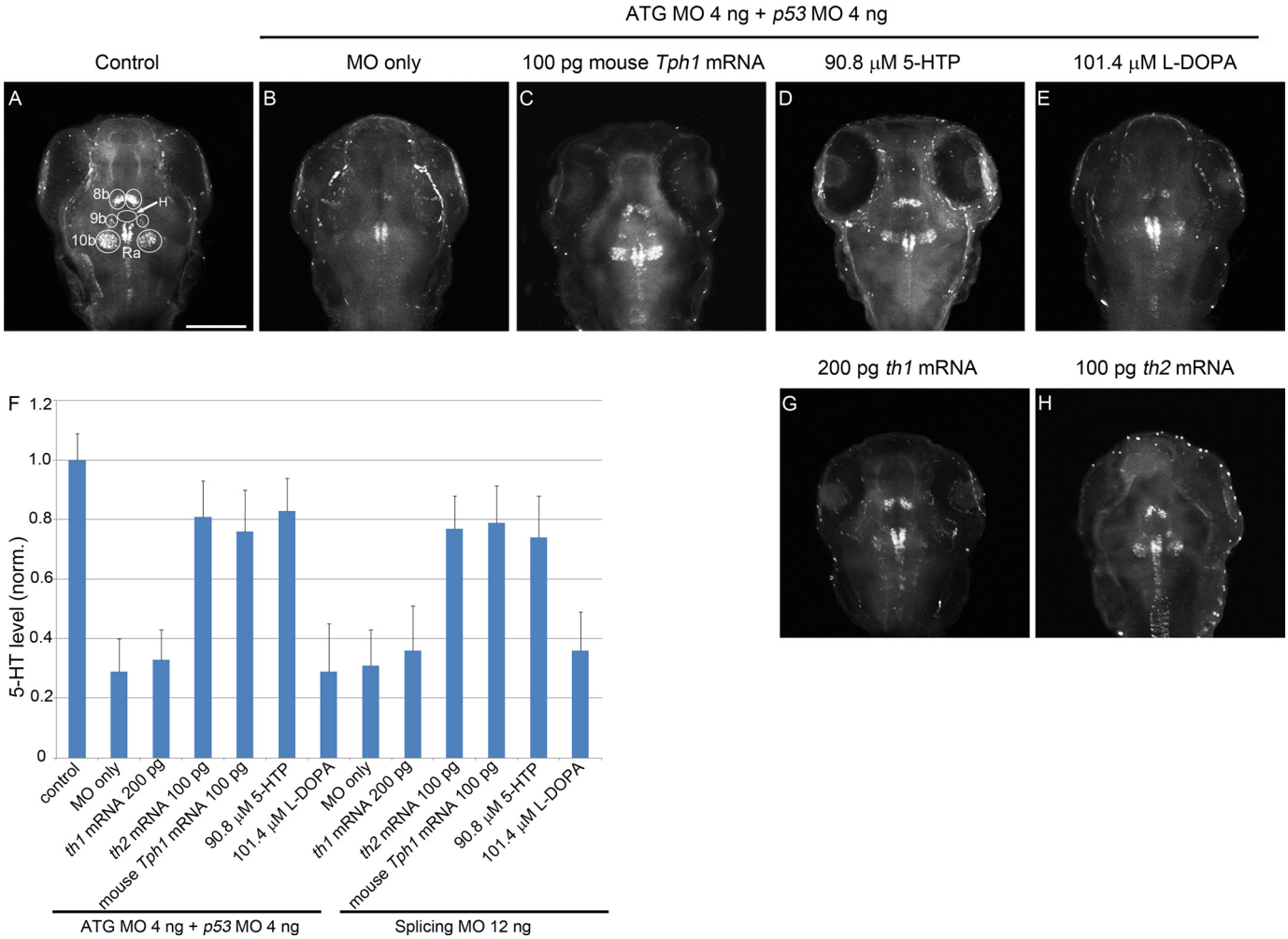

FIGURE 4. **Knockdown of *th2* causes reduction of 5-HT in the corresponding neurons, and this reduction can be rescued by both mRNA of *th2* and mouse *Tph1* as well as 5-HTP.** A *dorsal view* is shown, anterior to the *top*. *A–E*, *G*, and *H*, *z*-stack (70 μm) images of 5-HT immunoreactivity of 72 hpf embryos. The *white circles* indicate the regions of interest used for statistical analysis. *F*, statistical result of the mRNA and chemical rescue experiment in both morphant groups. The *y* axis shows relative 5-HT level. Both MOs generate significant reduction of the 5-HT level compared with control ($p < 0.05$). mRNA of *th2* and mouse *Tph1* and 5-HTP show significant rescue of 5-HT compared with both morphant groups ($p < 0.05$). In contrast, mRNA of *th1* and L-DOPA do not have a significant rescue effect in both morphant groups ($p > 0.05$). $n = 20$ in each group; *error bar*, S.E; *scale bar*, 100 μm. *White circles* indicate regions of interest. *H*, hypothalamic region immediately anterior to the raphe nucleus (*arrow*); *Ra*, raphe nucleus.

described previously (31), which were co-localized with 5-HT (Fig. 1, *S*, *V*, *W*, and *X*). Except for the 3b cluster, *th2*-positive neural clusters of 8b, 9b, and 10b co-localized with GFP-immunoreactive clusters of Pa, Hi, and Hc, respectively (Fig. 1, *S*, *T*, and *U*). Therefore, *th2* and 5-HT were co-localized at the ventral diencephalon and the caudal hypothalamus.

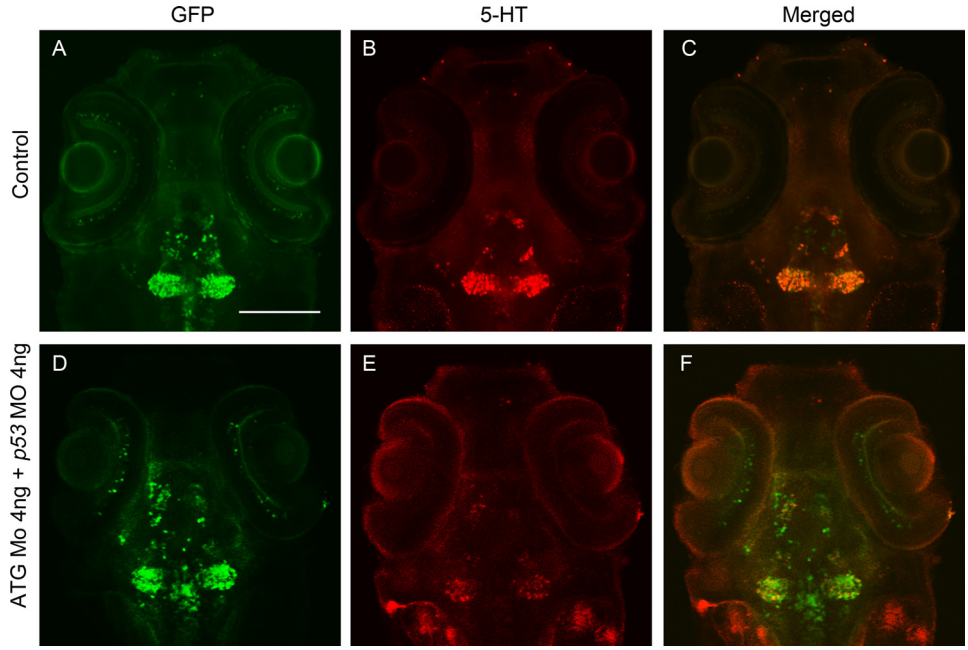

FIGURE 5. **Maximum intensity section of 5-HT in diencephalon and GFP immunoreactivity at 72 hpf shows that the decrease of 5-HT is not caused by cell loss.** A *dorsal view* is shown, anterior to the *top*. *A–C*, control embryo; *D–F*, ATG MO (4 ng) + *p53* MO (4 ng) embryo. The intensity of 5-HT in the morphant reduced sharply (*E*) compared with that of control (*B*), whereas the intensity of GFP in both groups did not change (*A* and *D*). *Scale bar*, 100 μm.

Knockdown of th2 Decreased the Level of 5-HT in the Corresponding Neurons—To functionally test if *th2* encoded an enzyme involved in 5-HT synthesis as a tryptophan hydroxylase, we first did a loss of function analysis of *th2* by antisense MOs. We designed two MOs, one splicing MO and one ATG MO (Table 1). The splicing MO targeted the boundary of exon 2 and intron 2-3 and caused either an insertion of intron 2–3 or an insertion of both intron 2-3 and intron 3-4. Both of these two splice variants would generate a truncated protein product putatively (Fig. 2*A*). The ATG MO blocked the translation of MO target site-EGFP fusion protein with high efficacy (Fig. 2*B*). To avoid the nonspecific apoptosis effect of the ATG MO (38), a *p53* MO was co-injected. Injection of *p53* MO by itself did not cause a decrease of 5-HT in 8b, 9b, and 10b *th2*-positive neurons (Fig. 3). In the morphant groups of both MOs, there was obvious reduction of the level of 5-HT in 8b, 9b, and 10b *th2*-positive neurons (Fig. 4*B*). To be concise, the result of splicing MO is not shown. Meanwhile, there was no obvious decrease of 5-HT in all of the other regions of the brain (*e.g.* the epiphysis (data not shown) and the raphe nucleus (Figs. 4, *B–H*)). This result also indicated that the reduction of 5-HT caused by knockdown of *th2* was specific. Moreover, we found that the *vmat2*-positive (GFP-immunoreactive) neurons in 8b, 9b, and 10b clusters were not affected, although the level of 5-HT decreased obviously (Fig. 5). This result excluded the possibility that the reduction of 5-HT was due to the loss of neurons. 5-HT immunoreactivity was evaluated in 8b, 9b, and 10b neurons using a semiquantitative method based on measurement of pixel grayscale values in regions of interest in confocal images. This showed ~50% decreases in 5-HT immunoreactivity in both ATG MO and splicing MO groups ($p = 0.001$ and 0.001, respectively; $n = 20$; Fig. 4*F*), suggesting that *th2* was indeed involved in the synthesis of 5-HT *in vivo*.

Mouse Tph1 mRNA and 5-HTP Rescued the Reduction of 5-HT—To rescue the reduction of 5-HT in 8b, 9b, and 10b clusters, injection of mRNA of *th1*, *th2*, and mouse *Tph1* was performed. We found that mRNA of the zebrafish *th2* and mouse *Tph1* could rescue, at least partially, the reduction of 5-HT to a level of higher than 70% of wild type ($p = 0.005$, 0.01, 0.006, and 0.001, respectively; $n = 20$), but the mRNA of *th1* could not ($p = 0.47$ and 0.27, respectively; $n = 20$) (Fig. 4, *C*, *F*, *G*, and *H*). This result indicated that *th2* had the same function of mouse *Tph1*, which was a tryptophan hydroxylase.

We also used the product of tryptophan hydroxylase, 5-HTP, and the product of tyrosine hydroxylase, L-DOPA, to rescue the reduction of 5-HT. We found that 5-HTP could partially rescue the reduction of 5-HT in both ATG MO and splicing MO groups ($p = 0.001$ and 0.013, respectively; $n = 20$), but L-DOPA could not ($p = 0.92$ and 0.43, respectively; $n = 20$) (Fig. 4, *D–F*). This result indicated that the reduction of 5-HT was due to a decrease of the supply of 5-HTP.

Th2 Had Tryptophan Hydroxylase Activity, Not Tyrosine Hydroxylase Activity, in Vitro—To test their tryptophan hydroxylase activity, Th2, Th1, and mouse TPH1 fused with a glutathione *S*-transferase (GST) tag were expressed in *E. coli*. All of these proteins were successfully expressed (Fig. 6*A*). With purified proteins, a commercial tryptophan hydroxylase detection kit from Genmed was used, in which tryptophan was the only substrate; thus, it could specifically measure tryptophan hydroxylase activity. We found that purified Th2 had a tryptophan hydroxylase activity of 14.4 ± 1.14 nM 5-HTP/min/mg, which was comparable with that of mouse TPH1 (17.6 ± 1.44 nM 5-HTP/min/mg, $p = 0.554$) (Fig. 6*B*). Both of them were more than 1 order of magnitude higher than that of the input control GST (0.58 ± 0.63 nM 5-HTP/min/mg, $p = 0.002$ and 0.000, respectively). In contrast, Th1 (0.13 ± 0.32 nM 5-HTP/

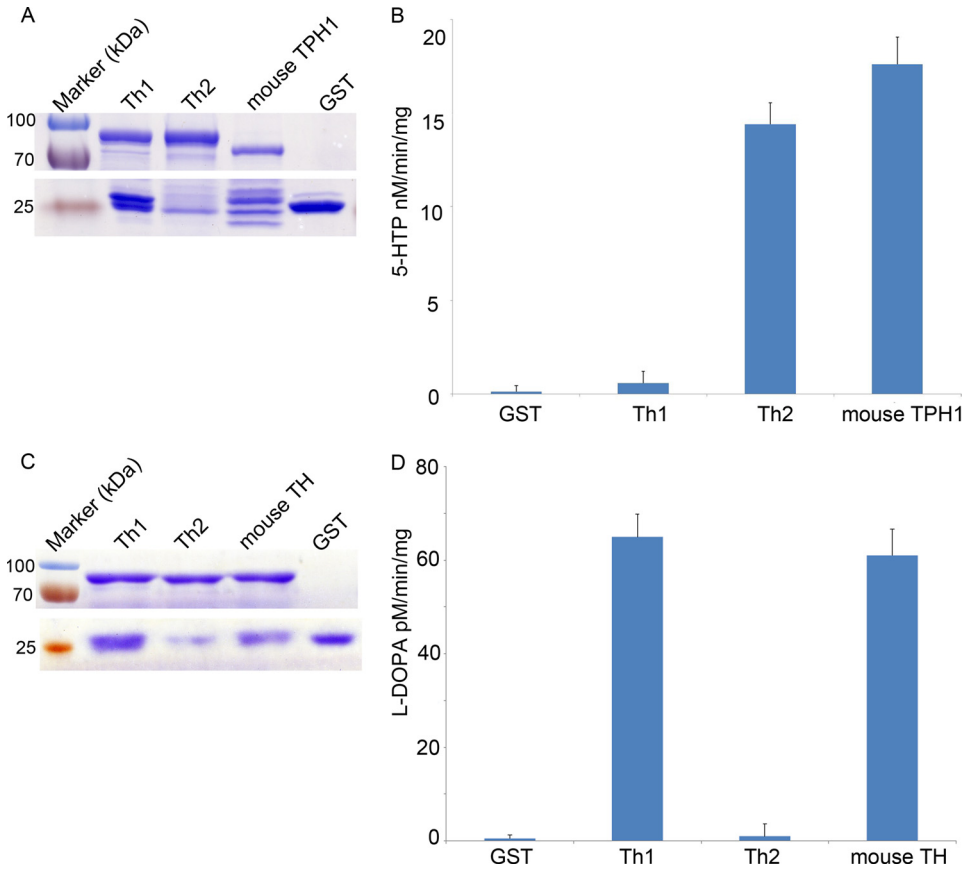

FIGURE 6. **Th2 has tryptophan hydroxylase activity, not tyrosine hydroxylase activity, *in vitro*.** *A*, Coomassie Brilliant Blue staining after protein purification shows that Th1, Th2, and mouse TPH1 express successfully (compare with the *GST lane*). *Top*, Th1, Th2, and mouse TPH1 tagged with GST. *Bottom*, GST expression of each group near a molecular mass of 25 kDa. *B*, tryptophan hydroxylase activity of GST, Th1, Th2, and mouse TPH1. There are no differences between the GST and Th1 groups ($p = 0.998$) or between the Th2 and mouse TPH1 groups ($p = 0.554$). In contrast, the activities of Th2 and mouse TPH1 are more than 1 order magnitude higher than that of GST ($p = 0.002$ and 0.000, respectively). *C*, Coomassie Brilliant Blue staining after protein purification shows that Th1, Th2, and mouse TH were expressed successfully (compare with the *GST lane*). *Top*, Th1, Th2, and mouse TH tagged with GST. *Bottom*, GST expression of each group near a molecular mass of 25 kDa. *D*, tyrosine hydroxylase activity of GST, Th1, Th2, and mouse TH. The tyrosine activity of Th1 and mouse TH is 65 ± 4.9 and 61 ± 5.6 pM L-DOPA/min/mg, respectively. There are no differences between the GST and Th2 groups ($p = 0.954$) or between the Th2 and mouse TH groups ($p = 0.464$). *Error bars*, S.E.

min/mg) did not have tryptophan hydroxylase activity, similar to that of GST ($p = 0.998$). These results indicated that Th2 had tryptophan hydroxylase activity *in vitro*, which was comparable with that of mouse TPH1.

To test whether Th2 has a tyrosine hydroxylase activity, we used a commercial tyrosine hydroxylase detection kit that was also from Genmed. The tyrosine hydroxylase activity of each protein above was measured using mouse TH as a positive control. We found that Th2 did not have tyrosine hydroxylase activity (1 ± 0.8 pM L-DOPA/min/mg) (Fig. 6, *C* and *D*). In contrast, Th1 had a tyrosine hydroxylase of 65 ± 4.9 pM L-DOPA/min/mg, which was comparable with the activity of mouse TH (61 ± 5.6, $p = 0.464$) (Fig. 6*D*). These results showed that Th1 had tyrosine hydroxylase activity, but Th2 did not. In summary, based on both *in vivo* and *in vitro* results, we concluded that zebrafish *th2* encoded a tryptophan hydroxylase and should be used as a marker gene of serotonergic neurons.

DISCUSSION

The zebrafish *th2* was thought to originate from gene duplication of *th*. The *th2* sequence is ~60% identical to mammalian *TH* sequence and 47% identical to the phenylalanine hydroxylase (*pah*) and *tph* sequences (25). Given that this duplication occurred far beyond teleost-specific third round whole genome duplication (28) and that teleost *th2* has twice the rate of nucleotide substitution as *th1* (25), there is a possibility that *th2* has evolved and preserved by neofunctionalization (25, 39). Both our *in vivo* and *in vitro* evidence indicates that *th2* obtains a novel tryptophan hydroxylase function.

Neuromodulatory DA neurons are destined to express *th*, *ddc*, *dat*, and *vmat* and contain dopamine. In the adult zebrafish brain, the expression pattern of these markers is not homogeneous, because dopamine-immunoreactive signal is weak in the olfactory bulb, telencephalon, pretectum, and preoptic nuclei, where highly irradiated tyrosine hydroxylase can be detected; in contrast, a high level of dopamine-immunoreactive signal with a low level of *ddc* can be detected in the paraventricular organ (29). To avoid this complexity, we used a zebrafish embryo in which the central nervous system is simpler than in the adult to investigate the relationship of *th2*, *vmat2*, and serotonin. We found that in the embryo, *th2* co-localizes with 5-HT except in the 3b cluster in preoptic region. Similarly, in the adult, a high level of *th2* can be detected in the preoptic region (29), but no 5-HT or a very low level of 5-HT can be detected in the 3b cluster, as described by Kaslin and Panula (37). One possibility

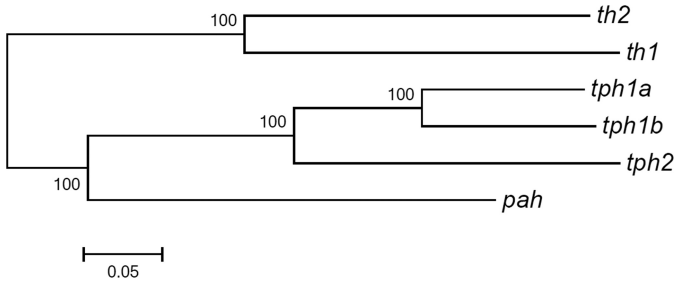

FIGURE 7. **Similarity dendrogram of zebrafish *th1*, *th2*, *pah*, and *tph* cluster genes using MEGA program.** Based on sequence homology, *th1* and *th2* clustered in one group, whereas the distance between *th1* and *tph* cluster genes is similar to that of *th2*. *pah* is used as an outside group.

is that these *th2*-positive neurons are immature and thus cannot synthesize the neurotransmitter. If so, why these immature neurons are kept not only in the embryo but also in the adult needs to be investigated further.

Although many cells contain 5-HT without synthesizing it, 5-HT is used as a marker to identify 5-HT neurons in zebrafish (6, 12, 30, 37, 40). *tph* can be used as a specific marker for 5-HT-producing neurons (41). In zebrafish, three genes coding for *tph* have been identified and designated as *tph1a*, *tph1b*, and *tph2*, respectively. Among them, *tph1a* expresses in epiphysis between 30 and 5 dpf (42), *tph1b* only expresses temporally from 10 to 16 hpf in the posterior axis (42) and transiently in the preoptic nucleus from 22 to 32 hpf (43), and *tph2* expresses in the epiphysis and the raphe nucleus from 24 to 5 dpf (44). None of them expresses at the diencephalic 5-HT neurons. Our finding that *th2* co-localizes with these 5-HT neurons and is responsible for the synthesis of 5-HT both *in vivo* and *in vitro* suggests that these diencephalic 5-HT neurons are 5-HT-producing neurons. As a tryptophan hydroxylase and thus a 5-HT neuron marker, *th2* needs to be redesignated. Considering that *th2* originates from the duplication of *th*, which is distinct from the other three *tph* genes (Fig. 7) (25), we suggest that *th2* be renamed as *tph3*.

With respect to neuronal development, the ventral diencephalic DA neurons and 5-HT neurons share a common transcriptional regulator, *Spt5*, whose mutation is called *foggy*. *foggy* exhibits reduction of DA neurons and a corresponding surplus of 5-HT neurons in the ventral diencephalon of zebrafish (6). According to our findings, these 5-HT neurons are *th2*-positive neurons and thus not only contain 5-HT but also produce it. Recently, a neurotrophic factor, called mesencephalic astrocyte-derived neurotrophic factor (*MANF*) has been found to be able to affect the expression of both *th1* and *th2* (45). This result indicates that DA and 5-HT neurons share a common neurotrophic factor. With respect to the PD-like model in zebrafish, knockdown of PTEN-induced putative kinase (*pink1*), whose mutation in humans can cause early onset PD (46), generates a reduction of *th1*- and *th2*-positive neurons in the ventral diencephalon, with a more severe decrease of *th2* than *th1* (17). Based on our findings, this result suggests that *th2*-positive 5-HT neurons are affected in a *pink1* knockdown PD-like model. In human PD, 5-HT neuron loss is found (47). Our finding implies that the zebrafish model of PD can exhibit loss of both DA neurons and 5-HT neurons.

Acknowledgments—We thank Danyang Wang and Xi Ren for critical discussions when this project was initiated. We also thank Ruibin Yan, Yanyan Ding, Zelin Chen, Jun Xu, and Lianbo Li for technical assistance and Chunfang Qin for zebrafish husbandry.

REFERENCES

1. Riederer, P., and Wuketich, S. (1976) Time course of nigrostriatal degeneration in Parkinson's disease. A detailed study of influential factors in human brain amine analysis. *J. Neural Transm.* **38,** 277–301
2. Hornykiewicz, O., and Kish, S. J. (1987) Biochemical pathophysiology of Parkinson's disease. *Adv. Neurol.* **45,** 19–34
3. Lees, A. J., Hardy, J., and Revesz, T. (2009) Parkinson's disease. *Lancet* **373,** 2055–2066
4. Iversen, S. D., and Iversen, L. L. (2007) Dopamine. 50 years in perspective. *Trends Neurosci.* **30,** 188–193
5. Guo, S., Wilson, S. W., Cooke, S., Chitnis, A. B., Driever, W., and Rosenthal, A. (1999) Mutations in the zebrafish unmask shared regulatory pathways controlling the development of catecholaminergic neurons. *Dev. Biol.* **208,** 473–487
6. Guo, S., Yamaguchi, Y., Schilbach, S., Wada, T., Lee, J., Goddard, A., French, D., Handa, H., and Rosenthal, A. (2000) A regulator of transcriptional elongation controls vertebrate neuronal development. *Nature* **408,** 366–369
7. Lee, S. A., Shen, E. L., Fiser, A., Sali, A., and Guo, S. (2003) The zebrafish forkhead transcription factor Foxi1 specifies epibranchial placode-derived sensory neurons. *Development* **130,** 2669–2679
8. Del Giacco, L., Sordino, P., Pistocchi, A., Andreakis, N., Tarallo, R., Di Benedetto, B., and Cotelli, F. (2006) Differential regulation of the zebrafish orthopedia 1 gene during fate determination of diencephalic neurons. *BMC Dev. Biol.* **6,** 50
9. Jeong, J. Y., Einhorn, Z., Mercurio, S., Lee, S., Lau, B., Mione, M., Wilson, S. W., and Guo, S. (2006) Neurogenin 1 is a determinant of zebrafish basal forebrain dopaminergic neurons and is regulated by the conserved zinc finger protein Tof/Fezl. *Proc. Natl. Acad. Sci. U.S.A.* **103,** 5143–5148
10. Blechman, J., Borodovsky, N., Eisenberg, M., Nabel-Rosen, H., Grimm, J., and Levkowitz, G. (2007) Specification of hypothalamic neurons by dual regulation of the homeodomain protein Orthopedia. *Development* **134,** 4417–4426
11. Bretaud, S., Allen, C., Ingham, P. W., and Bandmann, O. (2007) p53-dependent neuronal cell death in a DJ-1-deficient zebrafish model of Parkinson's disease. *J. Neurochem.* **100,** 1626–1635
12. Ryu, S., Mahler, J., Acampora, D., Holzschuh, J., Erhardt, S., Omodei, D., Simeone, A., and Driever, W. (2007) Orthopedia homeodomain protein is essential for diencephalic dopaminergic neuron development. *Curr. Biol.* **17,** 873–880
13. Anichtchik, O., Diekmann, H., Fleming, A., Roach, A., Goldsmith, P., and Rubinsztein, D. C. (2008) Loss of PINK1 function affects development and results in neurodegeneration in zebrafish. *J. Neurosci.* **28,** 8199–8207
14. Flinn, L., Mortiboys, H., Volkmann, K., Köster, R. W., Ingham, P. W., and Bandmann, O. (2009) Complex I deficiency and dopaminergic neuronal cell loss in parkin-deficient zebrafish (*Danio rerio*). *Brain* **132,** 1613–1623
15. Fett, M. E., Pilsl, A., Paquet, D., van Bebber, F., Haass, C., Tatzelt, J., Schmid, B., and Winklhofer, K. F. (2010) Parkin is protective against proteotoxic stress in a transgenic zebrafish model. *PLoS One* **5,** e11783
16. Mahler, J., Filippi, A., and Driever, W. (2010) DeltaA/DeltaD regulate multiple and temporally distinct phases of notch signaling during dopaminergic neurogenesis in zebrafish. *J. Neurosci.* **30,** 16621–16635
17. Sallinen, V., Kolehmainen, J., Priyadarshini, M., Toleikyte, G., Chen, Y. C., and Panula, P. (2010) Dopaminergic cell damage and vulnerability to MPTP in Pink1 knockdown zebrafish. *Neurobiol. Dis.* **40,** 93–101
18. Sheng, D., Qu, D., Kwok, K. H., Ng, S. S., Lim, A. Y., Aw, S. S., Lee, C. W., Sung, W. K., Tan, E. K., Lufkin, T., Jesuthasan, S., Sinnakaruppan, M., and Liu, J. (2010) Deletion of the WD40 domain of LRRK2 in zebrafish causes Parkinsonism-like loss of neurons and locomotive defect. *PLoS Genet.* **6,** e1000914
19. Xi, Y., Ryan, J., Noble, S., Yu, M., Yilbas, A. E., and Ekker, M. (2010)

Impaired dopaminergic neuron development and locomotor function in zebrafish with loss of pink1 function. *Eur. J. Neurosci.* **31,** 623–633
20. Ren, G., Xin, S., Li, S., Zhong, H., and Lin, S. (2011) Disruption of LRRK2 does not cause specific loss of dopaminergic neurons in zebrafish. *PLoS One* **6,** e20630
21. Rink, E., and Wullimann, M. F. (2001) The teleostean (zebrafish) dopaminergic system ascending to the subpallium (striatum) is located in the basal diencephalon (posterior tuberculum). *Brain Res.* **889,** 316–330
22. Rink, E., and Wullimann, M. F. (2002) Connections of the ventral telencephalon and tyrosine hydroxylase distribution in the zebrafish brain (*Danio rerio*) lead to identification of an ascending dopaminergic system in a teleost. *Brain Res. Bull.* **57,** 385–387
23. Tay, T. L., Ronneberger, O., Ryu, S., Nitschke, R., and Driever, W. (2011) Comprehensive catecholaminergic projectome analysis reveals single-neuron integration of zebrafish ascending and descending dopaminergic systems. *Nat. Commun.* **2,** 171
24. McKinley, E. T., Baranowski, T. C., Blavo, D. O., Cato, C., Doan, T. N., and Rubinstein, A. L. (2005) Neuroprotection of MPTP-induced toxicity in zebrafish dopaminergic neurons. *Brain Res. Mol. Brain Res.* **141,** 128–137
25. Candy, J., and Collet, C. (2005) Two tyrosine hydroxylase genes in teleosts. *Biochim. Biophys. Acta* **1727,** 35–44
26. Chen, Y. C., Priyadarshini, M., and Panula, P. (2009) Complementary developmental expression of the two tyrosine hydroxylase transcripts in zebrafish. *Histochem. Cell Biol.* **132,** 375–381
27. Filippi, A., Mahler, J., Schweitzer, J., and Driever, W. (2010) Expression of the paralogous tyrosine hydroxylase encoding genes *th1* and *th2* reveals the full complement of dopaminergic and noradrenergic neurons in zebrafish larval and juvenile brain. *J. Comp. Neurol.* **518,** 423–438
28. Yamamoto, K., Ruuskanen, J. O., Wullimann, M. F., and Vernier, P. (2010) Two tyrosine hydroxylase genes in vertebrates New dopaminergic territories revealed in the zebrafish brain. *Mol. Cell Neurosci.* **43,** 394–402
29. Yamamoto, K., Ruuskanen, J. O., Wullimann, M. F., and Vernier, P. (2011) Differential expression of dopaminergic cell markers in the adult zebrafish forebrain. *J. Comp. Neurol.* **519,** 576–598
30. McLean, D. L., and Fetcho, J. R. (2004) Ontogeny and innervation patterns of dopaminergic, noradrenergic, and serotonergic neurons in larval zebrafish. *J. Comp. Neurol.* **480,** 38–56
31. Wen, L., Wei, W., Gu, W., Huang, P., Ren, X., Zhang, Z., Zhu, Z., Lin, S., and Zhang, B. (2008) Visualization of monoaminergic neurons and neurotoxicity of MPTP in live transgenic zebrafish. *Dev. Biol.* **314,** 84–92
32. Westerfield, M. (2000) *The Zebrafish book: A Guide for the Laboratory Use of Zebrafish* (*Danio rerio*), 4th Ed., University of Oregon Press, Eugene, OR
33. Kimmel, C. B., Ballard, W. W., Kimmel, S. R., Ullmann, B., and Schilling, T. F. (1995) Stages of embryonic development of the zebrafish. *Dev. Dyn.* **203,** 253–310
34. Langheinrich, U., Hennen, E., Stott, G., and Vacun, G. (2002) Zebrafish as a model organism for the identification and characterization of drugs and genes affecting p53 signaling. *Curr. Biol.* **12,** 2023–2028
35. Yohrling, G. J., IV, Jiang, G. C., DeJohn, M. M., Robertson, D. J., Vrana, K. E., and Cha, J. H. (2002) Inhibition of tryptophan hydroxylase activity and decreased 5-HT1A receptor binding in a mouse model of Huntington's disease. *J. Neurochem.* **82,** 1416–1423
36. Brend, T., and Holley, S. A. (2009) Zebrafish whole mount high-resolution double fluorescent *in situ* hybridization. *J. Vis. Exp.*, doi: 10.3791/1229
37. Kaslin, J., and Panula, P. (2001) Comparative anatomy of the histaminergic and other aminergic systems in zebrafish (*Danio rerio*). *J. Comp. Neurol.* **440,** 342–377
38. Robu, M. E., Larson, J. D., Nasevicius, A., Beiraghi, S., Brenner, C., Farber, S. A., and Ekker, S. C. (2007) p53 activation by knockdown technologies. *PLoS Genet.* **3,** e78
39. Force, A., Lynch, M., Pickett, F. B., Amores, A., Yan, Y. L., and Postlethwait, J. (1999) Preservation of duplicate genes by complementary, degenerative mutations. *Genetics* **151,** 1531–1545
40. McLean, D. L., and Fetcho, J. R. (2004) Relationship of tyrosine hydroxylase and serotonin immunoreactivity to sensorimotor circuitry in larval zebrafish. *J. Comp. Neurol.* **480,** 57–71
41. Lillesaar, C. (2011) The serotonergic system in fish. *J. Chem. Neuroanat.* **41,** 294–308
42. Thisse, B., and Thisse, C. (2004) Fast Release Clones. A High Throughput Expression Analysis. *ZFIN Direct Data Submission* (http://zfin.org)
43. Bellipanni, G., Rink, E., and Bally-Cuif, L. (2002) Cloning of two tryptophan hydroxylase genes expressed in the diencephalon of the developing zebrafish brain. *Mech. Dev.* **119,** S215–S220
44. Rauch, G. J., Lyons, D. A., Middendorf, I., Friedlander, B., Arana, N., Reyes, T., and and Talbot, W. S. (2003) Submission and Curation of Gene Expression Data. *ZFIN Direct Data Submission* (http://zfin.org)
45. Chen, Y. C., Sundvik, M., Rozov, S., Priyadarshini, M., and Panula, P. (2012) MANF regulates dopaminergic neuron development in larval zebrafish. *Dev. Biol.* **370,** 237–249
46. Valente, E. M., Abou-Sleiman, P. M., Caputo, V., Muqit, M. M., Harvey, K., Gispert, S., Ali, Z., Del Turco, D., Bentivoglio, A. R., Healy, D. G., Albanese, A., Nussbaum, R., González-Maldonado, R., Deller, T., Salvi, S., Cortelli, P., Gilks, W. P., Latchman, D. S., Harvey, R. J., Dallapiccola, B., Auburger, G., and Wood, N. W. (2004) Hereditary early-onset Parkinson's disease caused by mutations in PINK1. *Science* **304,** 1158–1160
47. Halliday, G. M., Blumbergs, P. C., Cotton, R. G., Blessing, W. W., and Geffen, L. B. (1990) Loss of brainstem serotonin- and substance P-containing neurons in Parkinson's disease. *Brain Res.* **510,** 104–107